8-2009

EFFECTS OF PHASE AND AMPLITUDE ERRORS ON QAM SYSTEMS WITH ERROR-CONTROL CODING AND SOFT DECISION DECODING

Jason Ellis
Clemson University, jellis@clemson.edu

EFFECTS OF PHASE AND AMPLITUDE ERRORS ON QAM SYSTEMS WITH ERROR-CONTROL CODING AND SOFT-DECISION DECODING

A Thesis
Presented to
the Graduate School of
Clemson University

In Partial Fulfillment
of the Requirements for the Degree
Master of Science
Electrical Engineering

by
Jason D. Ellis
August 2009

Accepted by:
Dr. Michael Pursley, Committee Chair
Dr. Daniel Noneaker
Dr. Harlan Russell

ABSTRACT

Demodulation of M-ary quadrature amplitude modulation (M-QAM) requires the receiver to estimate the phase and amplitude of the received signal. The demodulator performance is sensitive to errors in these estimates, and the sensitivity increases as M increases. We examine the effects of phase and amplitude errors on the performance of QAM communication systems with error-control coding and soft-decision decoding. A mathematical analysis of these effects is presented for two soft-decision decoding metrics. Performance comparisons are given for 16-QAM and 64-QAM for two error-control coding techniques and two soft-decision decoding metrics.

ACKNOWLEDGMENTS

I would like to thank my advisor, Dr. Michael B. Pursley, for all of his assistance in the preparation of this thesis. I am very grateful for all of the guidance and support that he has given me during my graduate education, and I look forward to continued success working under his advisement. I would like to thank Dr. Daniel L. Noneaker and Dr. Harlan B. Russell for their generous efforts in serving on my committee. I am very grateful for the support that they have shown me and the roles that they have played in my success here at Clemson.

I would also like to thank family and friends for their love, prayers, and support. I am truly blessed to have such wonderful people in my life.

TABLE OF CONTENTS

Table of Contents (Continued)

Page

LIST OF TABLES

List of Tables (Continued)

Table Page

LIST OF FIGURES

List of Figures (Continued)

Figure Page

List of Figures (Continued)

Figure Page

CHAPTER 1
Introduction

We consider a communication system using M-ary quadrature amplitude modulation (M-QAM), also referred to as M-ary quadrature amplitude shift keying (M-QASK). This modulation technique is well known for its spectral efficiency, and it is often used for systems that operate with limited bandwidth. QAM requires coherent demodulation with accurate estimates of the phase and amplitude of received signals. The effect of a phase error on the performance of a coherent demodulator is investigated in [2] and [3], but the influence of error-control coding and soft-decision decoding was not examined. In this thesis we consider M-QAM systems that employ error-control coding and soft-decision decoding. We investigate the sensitivity of these systems to phase and amplitude errors at the receiver. A convolutional and turbo product code are employed for error-control coding for each of two soft-decision decoding metrics. The results of this research reveal how accurate the estimates of the phase and amplitude must be to maintain a certain performance in these systems.

The signal for M-QAM can be expressed as [2]

$$s(t, \varphi) = Au_i \cos(\omega_c t + \varphi) - Av_k \sin(\omega_c t + \varphi), 0 \leq t \leq T, \tag{1.1}$$

where A is the signal amplitude, ω_c is the frequency, T is the signal duration, and φ is the phase of the signal. In this thesis, the number of signals in the set is of the form $M = m^2$ for an even integer m. The variables u_i and v_k take on values from the

set $\{\pm 1, \pm 3, \ldots, \pm(m-1)\}$ [4]. If $M = 2^q$, q is an even integer, and $n = q/2$, then a *regular* M-QAM signal constellation consists of a square grid of uniformly spaced symbols in a 2^n by 2^n square array. Symbols in this type of constellation are called *nearest neighbors* if they are two adjacent symbols in the same row or column. A Gray code is a one-to-one assignment of binary words of length q to the symbols in a QAM constellation with the property that assignments for nearest neighbors disagree in exactly one bit position. There are many Gray codes for a given constellation, but we use the IEEE Standard Gray code for 16-QAM and 64-QAM [5]. The resulting constellations and bit assignments are referred to as *standard* 16-QAM and *standard* 64-QAM.

All results presented in this thesis are for an additive white Gaussian noise (AWGN) channel. A signal is sent over an AWGN channel and demodulated with a coherent inphase-quadrature correlation receiver. The outputs of the integrators in the receiver produce the decision statistic $\mathbf{Z} = (Z_1, Z_2)$, where Z_1 and Z_2 are independent Gaussian random variables. If $Z_1 = z_1$ and $Z_2 = z_2$, then we say the *received point* is $\mathbf{r} = (z_1, z_2)$. The correlators require perfect knowledge of the phase and amplitude of the received signals in order to use the maximum-likelihood decision regions. In practice, however, the receiver's estimates of the phase and amplitude are not perfectly accurate, and errors in these estimates degrade the performance of the system. In this thesis, we investigate the level of performance degradation caused by these types of errors.

CHAPTER 2
Phase and Amplitude Errors

2.1 Phase Error

A coherent correlation receiver used in a QAM system is shown in Fig. 2.1. A phase error in the system occurs if the phase φ of the received signal is not equal to the phase $\hat{\varphi}$ of the correlator's reference signal. The phase error is $\theta = \varphi - \hat{\varphi}$, and the output of the inphase correlator is [2]

$$\begin{aligned}
\hat{u}_i &= \int_0^T \left[Au_i \cos(\omega_c t + \varphi) - Av_k \sin(\omega_c t + \varphi)\right] \left[\sqrt{2}\cos(\omega_c t + \hat{\varphi})\right] dt \\
&= \sqrt{2}A \int_0^T u_i \cos(\omega_c t + \varphi)\cos(\omega_c t + \hat{\varphi}) - v_k \sin(\omega_c t + \varphi)\cos(\omega_c t + \hat{\varphi}) dt \\
&= \sqrt{2}A \int_0^T \frac{1}{2}\left[u_i \cos(\varphi - \hat{\varphi}) + u_i \cos(2\omega_c t + \varphi + \hat{\varphi})\right. \\
&\quad \left. - v_k \sin(\varphi - \hat{\varphi}) - v_k \sin(2\omega_c t + \varphi + \hat{\varphi})\right] dt \\
&= \frac{AT}{\sqrt{2}}(u_i \cos\theta - v_k \sin\theta). \qquad (2.1)
\end{aligned}$$

The double frequency terms in (2.1) have been neglected. Similarly, the output of the quadrature correlator is

$$\hat{v}_k = \frac{AT}{\sqrt{2}}(v_k \cos\theta + u_i \sin\theta). \qquad (2.2)$$

The received signals are rotated by the phase error θ, and the resulting output signal constellation is not in its original orientation. An example of a 16-QAM signal constellation is shown in Fig. 2.2. The signal constellation for a system with a perfect phase reference is shown as well as the constellation for a system with a 5° phase error. The maximum-likelihood decision boundaries for the system with a perfect

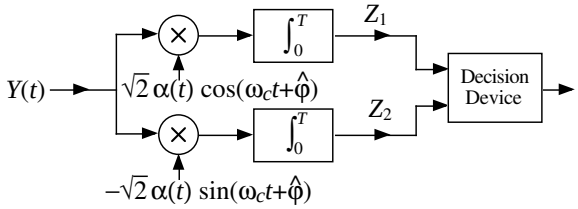

Figure 2.1: Inphase-quadrature coherent correlation receiver used for QAM demodulation.

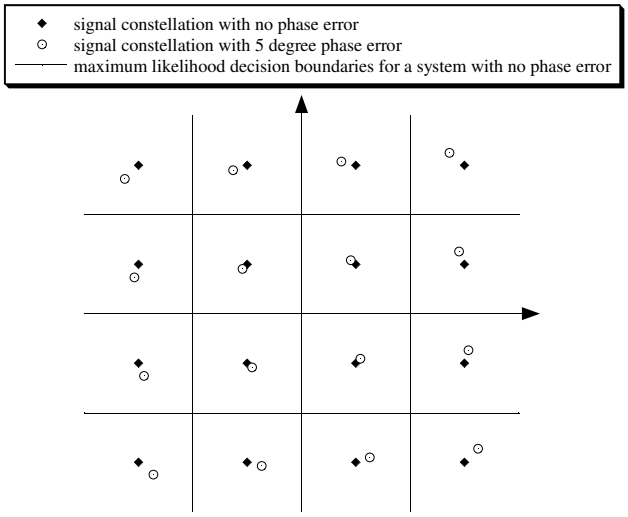

Figure 2.2: 16-QAM signal constellation and decision boundaries for a system with no phase error and a constellation with a 5° phase error.

phase reference are included. Each point in the rotated constellation is closer to at least one boundary, which causes an increase of incorrect bit decisions.

The effects of phase errors on QAM systems with no error-control coding have been investigated in [3] and [4]. The rotation of the received signals causes degradation in the performance of the system. An expression for the average symbol error probability for an M-QAM system with a phase error is presented in [3] and [4]. The average

symbol error probability as a function of θ is given by

$$\begin{aligned} P_E(\theta) &= \frac{4}{M}\sum_j\sum_l Q\{\Delta\,[l+(1-l)\cos\theta - j\sin\theta]\} \\ &\quad - \frac{4}{M}\sum_k\sum_l Q\{\Delta\,[k+(1-k)\cos\theta + (l-1)\sin\theta]\}\times \\ &\qquad\qquad Q\{\Delta\,[l+(1-l)\cos\theta - (k-1)\sin\theta]\}, \end{aligned} \tag{2.3}$$

where $Q(x) = \int_x^\infty (1/\sqrt{2\pi})\exp(-y^2/2)dy$, and Δ is related to the signal-to-noise ratio in [4]. For 16-QAM, $\Delta = \sqrt{4\mathcal{E}_b/5N_0}$, and for 64-QAM, $\Delta = \sqrt{2\mathcal{E}_b/7N_0}$, where $\mathcal{E}_b/N_0$ is the bit-energy-to-noise density ratio. The sums over j and l are for the values $j = \pm1, \pm3, \ldots, \pm(m-1)$ and $l = \pm2, \pm4, \ldots, \pm(m-1)$. The sums over k and l are for the values $k, l = 0, \pm2, \pm4, \ldots, \pm(m-2)$. Because of the symmetry in these sets and the behavior of the sine and cosine functions, the expression is symmetric about $\theta = 0$. Substituting $-\theta$ into (2.3) gives

$$\begin{aligned} P_E(\theta) &= \frac{4}{M}\sum_j\sum_l Q\{\Delta\,[l+(1-l)\cos\theta + j\sin\theta]\} \\ &\quad - \frac{4}{M}\sum_k\sum_l Q\{\Delta\,[k+(1-k)\cos\theta - (l-1)\sin\theta]\}\times \\ &\qquad\qquad Q\{\Delta\,[l+(1-l)\cos\theta + (k-1)\sin\theta]\}. \end{aligned} \tag{2.4}$$

Because the set of values for the variable j contains both the positive and negative values of each integer, the first double summation in this expression is equal to the first double summation in (2.3). Also, because k and l take on the same values, the second double summation in this expression is equal to the second double summation in (2.3). Thus, the two equations are equal, and the same symbol error probability is achieved for a phase error of θ or $-\theta$.

As the phase error is increased, the required signal-to-noise ratio to reach a given

symbol error probability is also increased. Table 2.1 shows the required bit-energy-to-noise density ratio to achieve a symbol error probability of 10^{-5} in a 16-QAM system with no error control coding [3], [4]. As the phase error is increased, the required value of ENR $= 10 \log_{10} (\mathcal{E}_b/N_0)$ also increases.

Table 2.1: Required ENR for a symbol error probability of 10^{-5} in a 16-QAM system.

Phase (deg)	Required ENR (dB)
0.0	14.02
2.5	14.72
5.0	16.13
7.5	17.93
10.0	20.31

2.2 Amplitude Error

The optimum correlator also requires knowledge of the amplitude of the received signal. An amplitude error in an M-QAM system will result if there is an unknown gain factor in the receiver's estimate of the signal amplitude. Let β represent the *gain factor* in the receiver's estimate of the amplitude. An error in the estimation of the amplitude or strength of the received signal results in a gain factor other than unity. If β is less than 1.0, the receiver under-estimates the amplitude. This type of error can be viewed as a contraction of the receiver's decision boundaries. If β is greater than 1.0, the receiver over-estimates the amplitude. This type of error can be viewed as an expansion of the receiver's decision boundaries. The resulting decision regions are not the maximum-likelihood decision regions. Fig. 2.3 is an example of a 16-QAM signal constellation and the maximum likelihood decision boundaries for a system with perfect amplitude knowledge. If $\beta = 1.1$, then Fig. 2.4 shows the receiver's estimate of the signal constellation and decision boundaries in Fig. 2.3. The receiver's estimates of the signal points and the decision boundaries are expanded by the gain factor β.

An amplitude error at the receiver also causes the system to have suboptimum performance. For 16-QAM, if β is not equal to unity, then the receiver's decision boundaries are at 0 and $\pm 2\beta$. As the error factor β is varied from unity, the required signal-to-noise ratio to reach a given symbol error probability is increased. Table 2.2 shows the required bit-energy-to-noise density ratio to achieve an average symbol error probability of 10^{-5} for several values of β.

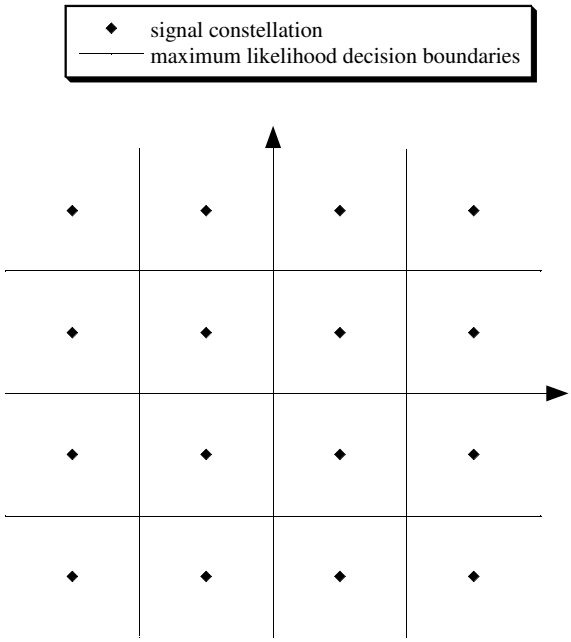

Figure 2.3: 16-QAM signal constellation and maximum likelihood decision boundaries.

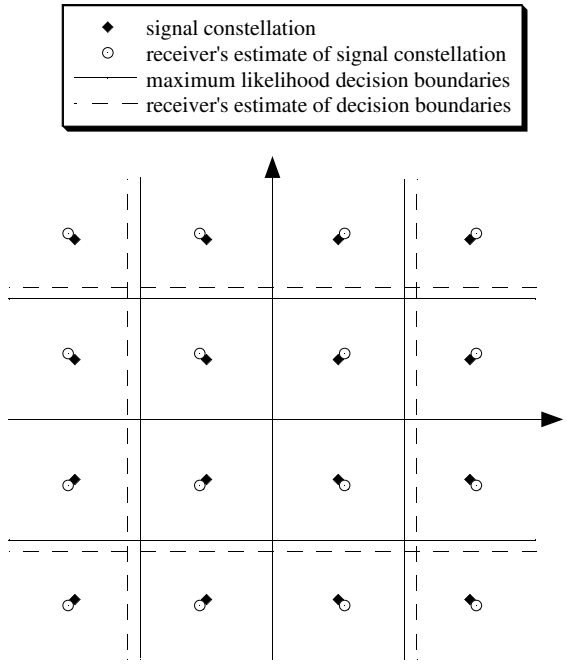

Figure 2.4: Receiver's estimate of a 16-QAM signal constellation and decision boundaries for a system with $\beta = 1.1$.

Table 2.2: Required ENR for a symbol error probability of 10^{-5} in a 16-QAM system.

Gain Factor (β)	Required ENR (dB)
0.85	16.65
0.9	15.53
0.95	14.55
1.0	14.03
1.05	14.55
1.1	15.53
1.15	16.65

CHAPTER 3
Log Likelihood Ratio Metric

One of the soft-decision metrics considered for decoding the received signals is a bit metric that uses the log likelihood ratio for each of the bit positions. The value of the ratio is used to decide what bits were sent and to place a quantitative measure of reliability on the bit decisions. The specifications of the metric depend on the Gray code being used in the system. For standard 16-QAM and 64-QAM, half of the bits depend on the horizontal component of the received point, z_1, and the other half depend on the vertical component, z_2. For 16-QAM, the set of coordinates used for the symbols in the output constellation are from the set $\{-3, -1, +1, +3\}$. These are the mean values of each coordinate of the vector decision statistic $\mathbf{Z} = (Z_1, Z_2)$ at the output of the receiver. The log likelihood ratios for each bit decision can be written in terms of two functions g_1 and g_2 [1] that are defined by

$$g_1(z) = \frac{\exp\{-(z+3)^2/2\sigma^2\} + \exp\{-(z+1)^2/2\sigma^2\}}{\exp\{-(z-3)^2/2\sigma^2\} + \exp\{-(z-1)^2/2\sigma^2\}} \tag{3.1}$$

and

$$g_2(z) = \frac{\exp\{-(z+3)^2/2\sigma^2\} + \exp\{-(z-3)^2/2\sigma^2\}}{\exp\{-(z+1)^2/2\sigma^2\} + \exp\{-(z-1)^2/2\sigma^2\}}. \tag{3.2}$$

For 16-QAM, the noise variance, σ^2, is given by [1]

$$\sigma^2 = \frac{5N_0}{\mathcal{E}_s} = \frac{5}{4r}\frac{N_0}{\mathcal{E}_b}, \tag{3.3}$$

where r is the code rate of the error-control code, $\mathcal{E}_s$ is the average energy per QAM symbol, and $\mathcal{E}_b$ is the average energy per information bit. The four log likelihood ratios are $L_1(\mathbf{r}) = \ln[g_1(z_1)]$, $L_2(\mathbf{r}) = \ln[g_2(z_1)]$, $L_3(\mathbf{r}) = \ln[g_1(z_2)]$, and $L_4(\mathbf{r}) = \ln[g_2(z_2)]$,

where L_i is used for the ith bit decision. These four ratios make up the log likelihood ratio (LLR) metric for 16-QAM.

The same concept can be applied to standard 64-QAM. The coordinates for the symbols in the 64-QAM signal constellation are taken from the set $\{-7, -5, -3, -1, +1, +3, +5, +7\}$, and the log likelihood ratios can be written in terms of three functions g_1, g_2, and g_3 that are defined by

$$g_1(z) = \frac{\exp\left\{\frac{-(z+7)^2}{2\sigma^2}\right\} + \exp\left\{\frac{-(z+5)^2}{2\sigma^2}\right\} + \exp\left\{\frac{-(z+3)^2}{2\sigma^2}\right\} + \exp\left\{\frac{-(z+1)^2}{2\sigma^2}\right\}}{\exp\left\{\frac{-(z-7)^2}{2\sigma^2}\right\} + \exp\left\{\frac{-(z-5)^2}{2\sigma^2}\right\} + \exp\left\{\frac{-(z-3)^2}{2\sigma^2}\right\} + \exp\left\{\frac{-(z-1)^2}{2\sigma^2}\right\}}, \tag{3.4}$$

$$g_2(z) = \frac{\exp\left\{\frac{-(z+7)^2}{2\sigma^2}\right\} + \exp\left\{\frac{-(z+5)^2}{2\sigma^2}\right\} + \exp\left\{\frac{-(z-5)^2}{2\sigma^2}\right\} + \exp\left\{\frac{-(z-7)^2}{2\sigma^2}\right\}}{\exp\left\{\frac{-(z+3)^2}{2\sigma^2}\right\} + \exp\left\{\frac{-(z+1)^2}{2\sigma^2}\right\} + \exp\left\{\frac{-(z-1)^2}{2\sigma^2}\right\} + \exp\left\{\frac{-(z-3)^2}{2\sigma^2}\right\}}, \tag{3.5}$$

and

$$g_3(z) = \frac{\exp\left\{\frac{-(z+7)^2}{2\sigma^2}\right\} + \exp\left\{\frac{-(z+1)^2}{2\sigma^2}\right\} + \exp\left\{\frac{-(z-1)^2}{2\sigma^2}\right\} + \exp\left\{\frac{-(z-7)^2}{2\sigma^2}\right\}}{\exp\left\{\frac{-(z+5)^2}{2\sigma^2}\right\} + \exp\left\{\frac{-(z+3)^2}{2\sigma^2}\right\} + \exp\left\{\frac{-(z-3)^2}{2\sigma^2}\right\} + \exp\left\{\frac{-(z-5)^2}{2\sigma^2}\right\}}. \tag{3.6}$$

In this case, σ^2 is given by

$$\sigma^2 = \frac{21N_0}{\mathcal{E}_s} = \frac{7}{2r}\frac{N_0}{\mathcal{E}_b}. \tag{3.7}$$

The six LLRs are $L_1(\mathbf{r}) = \ln[g_1(z_1)]$, $L_2(\mathbf{r}) = \ln[g_2(z_1)]$, $L_3(\mathbf{r}) = \ln[g_3(z_1)]$, $L_4(\mathbf{r}) = \ln[g_1(z_2)]$, $L_5(\mathbf{r}) = \ln[g_2(z_2)]$, and $L_6(\mathbf{r}) = \ln[g_3(z_2)]$. These metrics are used to make bit decisions and provide a measure of reliability for the bit decisions that can be used in soft-decision decoding.

3.1 Mathematical Analysis of a Phase Error

The LLR metric depends on the distances between the received point and the inphase and quadrature components of the signal constellation points. A phase error

in the system causes these distances to change. The LLR metrics depend on the fact that the x and y values of the signal constellation points come from the set $\{\pm 1, \pm 3, \ldots, \pm(m-1)\}$. In the event of a phase error, the rotated signal constellation points do not take on values from this set. However, there are straight lines connecting the rotated signal points. Equations for these lines can be determined using a simple point-slope method. These equations are in terms of the phase error θ, and can be used to replace the signal components in the LLR metrics. Applying this method to $L_1(\mathbf{r})$ results in the exponents of (3.1) taking on the form

$$l_1(\mathbf{r},\theta) = \frac{-(z_1 - z_2\tan\theta + 3\sqrt{2}\tan\theta\sin(\frac{3\pi}{4}-\theta) - 3\sqrt{2}\cos(\frac{3\pi}{4}-\theta))^2}{2\sigma^2}, \tag{3.8}$$

$$l_2(\mathbf{r},\theta) = \frac{-(z_1 - z_2\tan\theta + \sqrt{2}\tan\theta\sin(\frac{3\pi}{4}-\theta) - \sqrt{2}\cos(\frac{3\pi}{4}-\theta))^2}{2\sigma^2}, \tag{3.9}$$

$$l_3(\mathbf{r},\theta) = \frac{-(z_1 - z_2\tan\theta + 3\sqrt{2}\tan\theta\sin(\frac{\pi}{4}-\theta) - 3\sqrt{2}\cos(\frac{\pi}{4}-\theta))^2}{2\sigma^2}, \tag{3.10}$$

and

$$l_4(\mathbf{r},\theta) = \frac{-(z_1 - z_2\tan\theta + \sqrt{2}\tan\theta\sin(\frac{\pi}{4}-\theta) - \sqrt{2}\cos(\frac{\pi}{4}-\theta))^2}{2\sigma^2}. \tag{3.11}$$

For a phase error θ, the LLR metric for the first bit is

$$L_1(\mathbf{r},\theta) = \ln\left[\frac{\exp\{l_1(\mathbf{r},\theta)\} + \exp\{l_2(\mathbf{r},\theta)\}}{\exp\{l_3(\mathbf{r},\theta)\} + \exp\{l_4(\mathbf{r},\theta)\}}\right]. \tag{3.12}$$

The other metrics have similar forms that depend on z_1, z_2, and θ. These metrics are not symmetric about θ for a given received point; however, because of the symmetry of the regular QAM constellation, the average effects of a phase error on a system using the LLR metric are symmetric. For example, a phase error θ has opposite effects

on the first bit metric for mirrored symbols across the x-axis. So in the absence of noise, $L_1((z_1, z_2), \theta) = L_1((z_1, -z_2), -\theta)$. This is also true for the second bit metric, L_2. Similarly, a phase error has opposite effects on the third and fourth bit metrics for mirrored symbols across the y-axis. Thus, in the absence of noise, $L_3((z_1, z_2), \theta) = L_3((-z_1, z_2), -\theta)$ and $L_4((z_1, z_2), \theta) = L_4((-z_1, z_2), -\theta)$. This symmetry results in the same performance for a system using the LLR metric with a phase error of θ or $-\theta$.

The sensitivity of the LLR to phase errors can be investigated by determining the slopes of the lines tangent to the metric functions with respect to the variable θ. Differentiating the metrics with respect to θ shows the level of sensitivity to changes in phase. A phase error in any practical communication system is a small value, so the slope of interest is the slope at $\theta = 0$. Evaluating the derivatives at $\theta = 0$ provides a quantitative measure of sensitivity that can be used for comparison to other metrics.

The derivatives were evaluated for 16-QAM using eight possible received points. These points lie on a circle centered at the signal constellation point (1,1). They are spaced $\pi/4$ radians apart with a radius equal to one standard deviation of the noise in the system. Most received points fall within one standard deviation of the noise, so the majority of received points lie within this circle of test points. A depiction of these possible received points is shown in Fig. 3.1. A 4-QAM signal constellation is shown, but the received points can be placed around any symbol in a constellation of any size. Using these values for z_1 and z_2 and $\theta = 0$, eight slopes of the LLR metrics were calculated. The magnitudes of these slopes were then averaged to find the average magnitude of the slope at a phase error of zero. Table 3.1 shows the evaluated derivatives at the 8 possible received points. The results are shown for a bit-energy-to-noise density ratio of 2.0 dB.

If the received points lie near a corner point or other exterior point rather than an

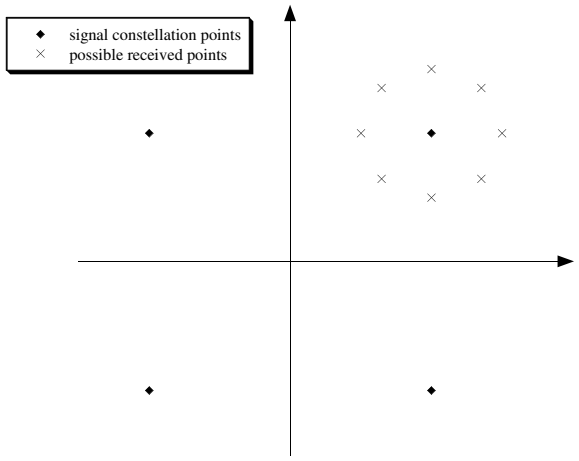

Figure 3.1: Possible received points near a QAM output signal.

Table 3.1: Slopes of LLR metrics for 16-QAM with zero phase error.

z_1	z_2	$L_1'(0)$	$L_2'(0)$	$L_3'(0)$	$L_4'(0)$
1.8881	1.8881	3.5233	-2.5887	-3.5233	2.5887
1	2.2559	.5509	-3.3014	-2.0096	1.3359
0.1119	1.8881	2.7481	-0.6682	-0.2088	0.1534
-0.2559	1	1.4618	0.757	0.4029	-0.3746
0.1119	0.1119	0.1629	-0.0396	-0.1629	0.0396
1	-0.2559	-0.4029	0.3746	-1.4618	-0.757
1.8881	0.1119	0.2088	-0.1534	-2.7481	0.6682
2.2559	1	2.0096	-1.3359	-3.5509	3.3014
Average (magnitude)		1.7585	1.1523	1.7585	1.1523

interior point, the magnitudes of the slopes are larger. The distance from the origin is proportional to the distance that a point moves due to a phase shift. Given a fixed value of θ, a received point near the corner point (3,3) moves a greater distance than a received point near the interior point (1,1). Table 3.2 displays the average magnitudes of slopes using received points near three different symbols, each of which is a different distance from the origin. The values in the table are for a bit-energy-to-noise density ratio of 2.0 dB.

As the signal-to-noise ratio increases, the magnitudes of the slopes of the tangent

Table 3.2: Average slope magnitudes of LLR metrics for 16-QAM with zero phase error.

type	(x,y) for symbol	Avg $\lvert L_1'(0)\rvert$	Avg $\lvert L_2'(0)\rvert$	Avg $\lvert L_3'(0)\rvert$	Avg $\lvert L_4'(0)\rvert$
interior	(1,1)	1.7585	1.1523	1.7585	1.1523
other ext.	(3,1)	2.3403	1.3958	4.9734	3.1761
corner	(3,3)	6.5872	3.9387	6.5872	3.9387

lines increase as well. This is due to the fact that the LLR metrics depend on the noise variance σ^2. As the signal-to-noise ratio increases, the output values for the LLR metrics increase in magnitude. A higher signal-to-noise ratio results in bit decisions with higher reliability. An increase in the magnitude of the slope suggests an increase in sensitivity to phase errors; however, the performance analysis of a coded system using the LLR metric does not reflect an increase in sensitivity to phase errors as the signal-to-noise ratio increases. So some type of normalization should be used to account for the increase in magnitude as the signal-to-noise ratio increases. One technique is to normalize the slope values by the magnitudes of the LLR metrics. In Tables 3.1 and 3.2, the derivatives of the metrics were evaluated at points near the symbol at (1,1). The signal constellation point (1,1) is also the mean value of the random decision statistic $\mathbf{Z}$, so $z_1 = 1$ and $z_2 = 1$ can be considered the most likely values for the variables z_1 and z_2 in the LLR metric functions. Dividing the slopes by the magnitudes of these functions at $(z_1, z_2) = (1, 1)$ and $\theta = 0$ normalizes the effects of the signal-to-noise ratio. Table 3.3 shows the average slope magnitudes for the interior point (1,1) in a 16-QAM system with zero phase error, and Table 3.4 shows these slopes normalized by the magnitudes of the LLR function values at $(z_1, z_2) = (1, 1)$. This same normalization technique was applied to the analysis of a corner point and other exterior point to give the normalized magnitudes in Tables 3.5 and 3.6.

Table 3.3: LLR slope magnitudes for an interior point in a 16-QAM system with zero phase error.

ENR (dB)	$\lvert L_1'(0)\rvert$	$\lvert L_2'(0)\rvert$	$\lvert L_3'(0)\rvert$	$\lvert L_4'(0)\rvert$
2	1.7585	1.1523	1.7585	1.1523
3	2.0489	1.4545	2.0489	1.4545
4	2.4043	1.7974	2.4043	1.7974
5	2.9065	2.5094	2.9065	2.5094
6	3.5171	3.3364	3.5171	3.3364
7	4.2672	4.2171	4.2672	4.2171
8	5.2133	5.2055	5.2133	5.2055
9	6.4373	6.4367	6.4373	6.4367
10	8.03	8.03	8.03	8.03

Table 3.4: Normalized LLR slope magnitudes for an interior point in a 16-QAM system with zero phase error.

ENR (dB)	norm $\lvert L_1'(0)\rvert$	norm $\lvert L_2'(0)\rvert$	norm $\lvert L_3'(0)\rvert$	norm $\lvert L_4'(0)\rvert$
2	1.1772	0.7714	1.1772	0.7714
3	1.1560	0.8206	1.1560	0.8206
4	1.1273	0.8427	1.1273	0.8427
5	1.1153	0.9629	1.1153	0.9629
6	1.0905	1.0344	1.0905	1.0344
7	1.0595	1.0471	1.0595	1.0471
8	1.0315	1.0300	1.0315	1.0300
9	1.0127	1.0126	1.0127	1.0126
10	1.0037	1.0037	1.0037	1.0037

The normalized slope values for 16-QAM suggest that metrics for corner points and other exterior points are more sensitive to phase errors than metrics for interior points. Also for corner points and other exterior points, some bit decisions are more sensitive to phase errors than others. Though the derivative analysis does not give a conclusive result on the sensitivity of the LLR to phase errors, it does provide some insight into the behavior of the LLR in an M-QAM system with a phase error.

Table 3.5: Normalized LLR slope magnitudes for a corner point in a 16-QAM system with zero phase error.

ENR (dB)	norm $\lvert L_1'(0)\rvert$	norm $\lvert L_2'(0)\rvert$	norm $\lvert L_3'(0)\rvert$	norm $\lvert L_4'(0)\rvert$
2	1.2387	3.1614	1.2387	3.1614
3	1.2889	3.0634	1.2889	3.0634
4	1.3359	3.0199	1.3359	3.0199
5	1.3789	3.0047	1.3789	3.0047
6	1.4174	3.0008	1.4174	3.0008
7	1.4502	3.0001	1.4502	3.0001
8	1.4749	3.0000	1.4749	3.0000
9	1.4901	3.0000	1.4901	3.0000
10	1.4972	3.0000	1.4972	3.0000

Table 3.6: Normalized LLR slope magnitudes for an other exterior point in a 16-QAM system with zero phase error.

ENR (dB)	norm $\lvert L_1'(0)\rvert$	norm $\lvert L_2'(0)\rvert$	norm $\lvert L_3'(0)\rvert$	norm $\lvert L_4'(0)\rvert$
2	0.4401	1.1203	3.3293	2.1262
3	0.4429	1.0514	3.3731	2.3697
4	0.4453	1.0066	3.3818	2.5280
5	0.4596	1.0016	3.3460	2.8888
6	0.4725	1.0003	3.2714	3.1033
7	0.4834	1.0000	3.1786	3.1413
8	0.4916	1.0000	3.0945	3.0899
9	0.4967	1.0000	3.0382	3.0379
10	0.4991	1.0000	3.0111	3.0111

3.2 Mathematical Analysis of an Amplitude Error

An amplitude error in an M-QAM system causes the distances used in the LLR metrics to change. If there is an amplitude error, then the receiver over-estimates or under-estimates the amplitude of the received signals, which leads to the values in the metrics being from the set $\{\pm\beta, \pm 3\beta, \ldots, \pm(m-1)\beta\}$ instead of the set $\{\pm 1, \pm 3, \ldots, \pm(m-1)\}$. The LLR metrics for a 16-QAM system with an amplitude

error are

$$L_1(\mathbf{r},\beta) = \ln\left[\frac{\exp\{-(z_1+3\beta)^2/2\sigma^2\}+\exp\{-(z_1+\beta)^2/2\sigma^2\}}{\exp\{-(z_1-3\beta)^2/2\sigma^2\}+\exp\{-(z_1-\beta)^2/2\sigma^2\}}\right], \tag{3.13}$$

$$L_2(\mathbf{r},\beta) = \ln\left[\frac{\exp\{-(z_1+3\beta)^2/2\sigma^2\}+\exp\{-(z_1-3\beta)^2/2\sigma^2\}}{\exp\{-(z_1+\beta)^2/2\sigma^2\}+\exp\{-(z_1-\beta)^2/2\sigma^2\}}\right], \tag{3.14}$$

$$L_3(\mathbf{r},\beta) = \ln\left[\frac{\exp\{-(z_2+3\beta)^2/2\sigma^2\}+\exp\{-(z_2+\beta)^2/2\sigma^2\}}{\exp\{-(z_2-3\beta)^2/2\sigma^2\}+\exp\{-(z_2-\beta)^2/2\sigma^2\}}\right], \tag{3.15}$$

and

$$L_4(\mathbf{r},\beta) = \ln\left[\frac{\exp\{-(z_2+3\beta)^2/2\sigma^2\}+\exp\{-(z_2-3\beta)^2/2\sigma^2\}}{\exp\{-(z_2+\beta)^2/2\sigma^2\}+\exp\{-(z_2-\beta)^2/2\sigma^2\}}\right]. \tag{3.16}$$

The sensitivity of the LLR metric to amplitude errors can be investigated by determining the slope of the functions in (3.13)–(3.16) with respect to the variable β. For an amplitude error, the slope of interest is the slope at $\beta = 1$. The same type of analysis that is described in Section 3.1 was performed for an amplitude error. The derivatives were evaluated using eight possible received points lying on a circle centered at the signal constellation point (1,1). Using these values for z_1 and z_2 and $\beta = 1$, eight slopes of the LLR metrics were calculated. The magnitudes of these slopes were then averaged to find the average magnitude of the slope at $\beta = 1$. Table 3.7 shows the evaluated derivatives at the eight received points using a bit-energy-to-noise density ratio of 2.0 dB.

The magnitudes of the slopes again have a strong dependence on the signal-to-noise ratio. As seen in Table 3.8, larger values of $\mathcal{E}_b/N_0$ result in larger magnitudes for the slopes of the LLR metrics. The same method described in Section 3.1 for normalizing the effects of the signal-to-noise ratio is employed, and the results for an interior point are shown in Table 3.9.

Table 3.7: Slopes of LLR metrics with a gain factor of unity.

z_1	z_2	$L_1'(1)$	$L_2'(1)$	$L_3'(1)$	$L_4'(1)$
1.8881	1.8881	1.2035	2.4830	1.2035	2.4830
1.0000	2.2559	0.5708	3.6082	1.6126	2.0580
0.1119	1.8881	0.0648	5.0321	1.2035	2.4830
-0.2559	1.0000	-0.1480	4.8779	0.5708	3.6082
0.1119	0.1119	0.0648	5.0321	0.0648	5.0321
1.0000	-0.2559	0.5708	3.6082	-0.1480	4.8779
1.8881	0.1119	1.2035	2.4830	0.0648	5.0321
2.2559	1.0000	1.6126	2.0580	0.5708	3.6082
Average (magnitude)		0.6798	3.6478	0.6798	3.6478

Table 3.8: LLR slope magnitudes for an interior point in a 16-QAM system with a gain factor of unity.

ENR (dB)	$\lvert L_1'(1)\rvert$	$\lvert L_2'(1)\rvert$	$\lvert L_3'(1)\rvert$	$\lvert L_4'(1)\rvert$
2	0.6798	3.6478	0.6798	3.6478
3	0.8487	4.6789	0.8487	4.6789
4	1.1406	5.9492	1.1406	5.9492
5	1.6492	7.5126	1.6492	7.5126
6	2.3853	9.4603	2.3853	9.4603
7	3.3782	11.9281	3.3782	11.9281
8	4.6356	15.0651	4.6356	15.0651
9	6.1458	19.0205	6.1458	19.0205
10	7.9230	23.9830	7.9230	23.9830

The same analysis for the corner point (3,3) and the other exterior point (3,1) shows that corner points appear to be less sensitive to amplitude errors than interior and other exterior points. Results in Tables 3.9, 3.10, and 3.11 do not completely reveal the effects of amplitude errors on the performance of the system. The level of sensitivity appears to be similar to that of phase errors, and sensitivity also depends on what symbol is sent. Interior points, corner points, and other exterior points are affected differently by phase and amplitude errors, and certain bit decisions tend to be more sensitive than others. The same analysis could be performed for 64-QAM;

Table 3.9: Normalized LLR slope magnitudes for an interior point in a 16-QAM system with a gain factor of unity.

ENR (dB)	norm $\lvert L_1'(1)\rvert$	norm $\lvert L_2'(1)\rvert$	norm $\lvert L_3'(1)\rvert$	norm $\lvert L_4'(1)\rvert$
2	0.4551	2.4419	0.4551	2.4419
3	0.4788	2.6398	0.4788	2.6398
4	0.5348	2.7892	0.5348	2.7892
5	0.6329	2.8829	0.6329	2.8829
6	0.7395	2.9331	0.7395	2.9331
7	0.8388	2.9617	0.8388	2.9617
8	0.9172	2.9808	0.9172	2.9808
9	0.9669	2.9924	0.9669	2.9924
10	0.9903	2.9977	0.9903	2.9977

Table 3.10: Normalized LLR slope magnitudes for a corner point in a 16-QAM system with a gain factor of unity.

ENR (dB)	norm $\lvert L_1'(1)\rvert$	norm $\lvert L_2'(1)\rvert$	norm $\lvert L_3'(1)\rvert$	norm $\lvert L_4'(1)\rvert$
2	0.5859	1.0065	0.5859	1.0065
3	0.5785	1.0005	0.5785	1.0005
4	0.5683	0.9886	0.5683	0.9886
5	0.5548	0.9970	0.5548	0.9970
6	0.5393	0.9995	0.5393	0.9995
7	0.5243	0.9999	0.5243	0.9999
8	0.5122	1.0000	0.5122	1.0000
9	0.5048	1.0000	0.5048	1.0000
10	0.5013	1.0000	0.5013	1.0000

however, because of the inconclusive results of the mathematical analysis, simulations are used for the investigation of 64-QAM.

Table 3.11: Normalized LLR slope magnitudes for an other exterior point in a 16-QAM system with a gain factor of unity.

ENR (dB)	norm $\lvert L_1'(1)\rvert$	norm $\lvert L_2'(1)\rvert$	norm $\lvert L_3'(1)\rvert$	norm $\lvert L_4'(1)\rvert$
2	0.5859	0.8394	0.1278	2.4419
3	0.5785	0.8964	0.1292	2.6398
4	0.5683	0.9303	0.1397	2.7892
5	0.5548	0.9676	0.1618	2.8829
6	0.5393	0.9869	0.1866	2.9331
7	0.5243	0.9955	0.2104	2.9617
8	0.5122	0.9987	0.2295	2.9808
9	0.5048	0.9997	0.2418	2.9924
10	0.5013	1.0000	0.2476	2.9977

CHAPTER 4

Distance Metric

Another soft-decision metric considered for decoding received signals is referred to as the distance metric [1]. This bit metric compares the distances from a received point to the nearest symbols in the output constellation in order to make bit decisions. If $\mathbf{r} = (z_1, z_2)$ is the received point, then the symbol s_0 is the symbol in the output constellation that is closest to the received point $\mathbf{r}$. The bits assigned to symbol s_0 are the bit decisions. The distance from the received point to the symbol s_0 is denoted by d_0. Now consider all symbols such that the ith bit differs from the ith bit of s_0. Of these symbols, the closest to the received point is denoted by s_i, and let d_i be the distance from the received point to the symbol s_i. If d_i is much greater than d_0, then the received point is far away from any symbols that differ from s_0 in the ith bit. So the reliability for the ith bit decision should be high if $d_i - d_0$ is large. Thus, the reliability measure for each bit decision is $d_i - d_0$, and these functions make up the distance metric. Because each symbol has different neighbors, the bit metrics will be different depending on where the received point falls. For 16-QAM, if the received point falls closest to the symbol at the interior point (1,1), then the distances used for the distance metric are

$$d_0(\mathbf{r}) = \sqrt{(z_1 - 1)^2 + (z_2 - 1)^2}, \tag{4.1}$$

$$d_1(\mathbf{r}) = \sqrt{(z_1 + 1)^2 + (z_2 - 1)^2}, \tag{4.2}$$

$$d_2(\mathbf{r}) = \sqrt{(z_1 - 3)^2 + (z_2 - 1)^2}, \tag{4.3}$$

$$d_3(\mathbf{r}) = \sqrt{(z_1 - 1)^2 + (z_2 + 1)^2}, \tag{4.4}$$

and

$$d_4(\mathbf{r}) = \sqrt{(z_1 - 1)^2 + (z_2 - 3)^2}. \tag{4.5}$$

The metrics used for bit decisions are $D_1(\mathbf{r}) = d_1 - d_0$, $D_2(\mathbf{r}) = d_2 - d_0$, $D_3(\mathbf{r}) = d_3 - d_0$, and $D_4(\mathbf{r}) = d_4 - d_0$. The symbols used for these distances are all nearest neighbors of the symbol at (1,1); however, this is not always the case. For example, if the received point falls closest to the corner point (3,3), then there are no nearest neighbors that differ in the first or third bits, so symbols that lie beyond nearest neighbors must be used for these bit decisions. If the distance metric is applied to 64-QAM, there are always bit decisions that require the use of symbols beyond nearest neighbors.

4.1 Mathematical Analysis of a Phase Error

Recall that a phase error rotates the received signal constellation points by an angle θ. The distance metric depends on the distances from the received point to the signal constellation points, so rotating these signals will cause these distances to change. A QAM signal constellation occupies a two dimensional space and can be represented by points in the complex plane. For example, the signal at the point (1,1) can be represented by the complex value $1 + j$ or $\sqrt{2}\exp(j\pi/4)$. Given a phase error, θ, the angle θ is added to the phase of this signal point, and the signal becomes $\sqrt{2}\exp(j\pi/4 + \theta)$. The distances for the distance metric can then be viewed as the magnitudes of vectors connecting a complex received point $\tilde{r} = z_1 + \mathrm{j}z_2$ and rotated versions of the signal constellation points. If this principle is applied to 16-QAM at the interior point located at $\sqrt{2}\exp(j\pi/4 + \theta)$, then (4.1)–(4.5) become

$$d_0(\mathbf{r}, \theta) = \sqrt{(z_1 - \sqrt{2}\cos(\pi/4 + \theta))^2 + (z_2 - \sqrt{2}\sin(\pi/4 + \theta))^2}, \tag{4.6}$$

$$d_1(\mathbf{r},\theta) = \sqrt{(z_1 - \sqrt{2}\cos(3\pi/4+\theta))^2 + (z_2 - \sqrt{2}\sin(3\pi/4+\theta))^2}, \tag{4.7}$$

$$d_2(\mathbf{r},\theta) = \sqrt{(z_1 - \sqrt{10}\cos(\tan^{-1}(1/3)+\theta))^2 + (z_2 - \sqrt{10}\sin(\tan^{-1}(1/3)+\theta))^2}, \tag{4.8}$$

$$d_3(\mathbf{r},\theta) = \sqrt{(z_1 - \sqrt{2}\cos(7\pi/4+\theta))^2 + (z_2 - \sqrt{2}\sin(7\pi/4+\theta))^2}, \tag{4.9}$$

and

$$d_4(\mathbf{r},\theta) = \sqrt{(z_1 - \sqrt{10}\cos(\tan^{-1}(3)+\theta))^2 + (z_2 - \sqrt{10}\sin(\tan^{-1}(3)+\theta))^2}. \tag{4.10}$$

Using the argument from Section 3.1, the symmetry of the QAM constellation causes the overall effects of a phase error on the distance metric to be symmetric. For each symbol in the constellation, there is a mirrored symbol that has an opposing effect for a given phase error. Thus, on average, a system with phase error θ will have the same performance as a system with phase error $-\theta$.

The mathematical analysis from Chapter 3 was performed to investigate the sensitivity of the distance metric to phase errors. The distances in (4.6)–(4.10) are differentiable with respect to θ. The derivatives were evaluated using eight possible received points lying on a circle centered at (1,1) with a radius equal to one standard deviation of the noise. Using the eight test points and $\theta = 0$, eight slopes of the lines tangent to the distance metrics were calculated. The magnitudes of these slopes were then averaged to find the average magnitude of the slope at a phase error of zero. Table 4.1 shows the evaluated derivatives at eight different received points using a bit-energy-to-noise density ratio of 2.0 dB. Table 4.2 shows the results for several values of $\mathcal{E}_b/N_0$ at this interior point.

The distance metric is not as heavily dependent on the signal-to-noise ratio as the LLR metric. The average slope magnitudes are approximately the same for all

Table 4.1: Slopes of distance metrics with zero phase error.

z_1	z_2	$D_1'(0)$	$D_2'(0)$	$D_3'(0)$	$D_4'(0)$
1.8881	1.8881	3.5233	-2.5887	-3.5233	2.5887
1	2.2559	.5509	-3.3014	-2.0096	1.3359
0.1119	1.8881	2.7481	-0.6682	-0.2088	0.1534
-0.2559	1	1.4618	0.757	0.4029	-0.3746
0.1119	0.1119	0.1629	-0.0396	-0.1629	0.0396
1	-0.2559	-0.4029	0.3746	-1.4618	-0.757
1.8881	0.1119	0.2088	-0.1534	-2.7481	0.6682
2.2559	1	2.0096	-1.3359	-3.5509	3.3014
Average (magnitude)		1.2553	0.896	1.2553	0.896

Table 4.2: Distance metric slope magnitudes for an interior point in a 16-QAM system with zero phase error.

ENR (dB)	$\lvert D_1'(0)\rvert$	$\lvert D_2'(0)\rvert$	$\lvert D_3'(0)\rvert$	$\lvert D_4'(0)\rvert$
2	1.2553	0.896	1.2553	0.896
3	1.253	0.9178	1.253	0.9178
4	1.2477	0.9351	1.2477	0.9351
5	1.2405	0.9488	1.2405	0.9488
6	1.2321	0.9596	1.2321	0.9596
7	1.223	0.9681	1.223	0.9681
8	1.2137	0.9748	1.2137	0.9748
9	1.2046	0.98	1.2046	0.98
10	1.1958	0.9842	1.1958	0.9842

values of $\mathcal{E}_b/N_0$ in Table 4.2. This is also true for corner points and other exterior points, as seen in Tables 4.3 and 4.4, so no normalization techniques are needed. As with the LLR metric, the distance metrics that involve corner points and other exterior points appear to be more sensitive to changes in phase than the metrics for interior points. However, unlike the LLR metric, there appears to be little variation among the sensitivity of different bit decisions. The slope magnitudes from Tables 4.2, 4.3, and 4.4 are often fairly close in value to the normalized slopes of the LLR metrics in Tables 3.4, 3.5, and 3.6. This suggests that the LLR and distance metrics

Table 4.3: Distance metric slope magnitudes for a corner point in a 16-QAM system with zero phase error.

ENR (dB)	$\lvert D_1'(0)\rvert$	$\lvert D_2'(0)\rvert$	$\lvert D_3'(0)\rvert$	$\lvert D_4'(0)\rvert$
2	3.4014	2.9584	3.4014	2.9584
3	3.3969	3.0243	3.3969	3.0243
4	3.3916	3.0773	3.3916	3.0773
5	3.3858	3.1196	3.3858	3.1196
6	3.38	3.1534	3.38	3.1534
7	3.3742	3.1805	3.3742	3.1805
8	3.3686	3.2023	3.3686	3.2023
9	3.3633	3.22	3.3633	3.22
10	3.3584	3.2344	3.3584	3.2344

Table 4.4: Distance metric slope magnitudes for an other exterior point in a 16-QAM system with zero phase error.

ENR (dB)	$\lvert D_1'(0)\rvert$	$\lvert D_2'(0)\rvert$	$\lvert D_3'(0)\rvert$	$\lvert D_4'(0)\rvert$
2	2.2488	1.6982	2.7518	2.688
3	2.2287	1.7334	2.8072	2.7534
4	2.2106	1.7664	2.8499	2.8054
5	2.1944	1.7968	2.8823	2.8465
6	2.1799	1.8244	2.9067	2.8788
7	2.167	1.8495	2.9249	2.9043
8	2.1555	1.872	2.9383	2.9243
9	2.1452	1.8923	2.9481	2.9401
10	2.136	1.9104	2.9551	2.9526

have about the same level of sensitivity to phase errors. This is confirmed in the performance analysis discussed in Chapter 5, which shows very little difference in sensitivity to phase errors between the LLR and distance metrics. The mathematical analysis does not provide any conclusive observations on the behavior of these metrics in the presence of phase errors; however, it does serve as a useful tool to supplement observations made from simulation.

4.2 Mathematical Analysis of an Amplitude Error

An amplitude error also affects the distance metrics. Given a gain factor β, the receiver over-estimates or under-estimates the amplitude of the received signals such that the values used for the distances are from the set $\{\pm\beta, \pm 3\beta, \ldots, \pm(m-1)\beta\}$. So the interior point (1,1) is assumed to be located at (β, β). Thus, (4.1)–(4.5) for 16-QAM become

$$d_0(\mathbf{r}, \beta) = \sqrt{(z_1 - \beta)^2 + (z_2 - \beta)^2}, \tag{4.11}$$

$$d_1(\mathbf{r}, \beta) = \sqrt{(z_1 + \beta)^2 + (z_2 - \beta)^2}, \tag{4.12}$$

$$d_2(\mathbf{r}, \beta) = \sqrt{(z_1 - 3\beta)^2 + (z_2 - \beta)^2}, \tag{4.13}$$

$$d_3(\mathbf{r}, \beta) = \sqrt{(z_1 - \beta)^2 + (z_2 + \beta)^2}, \tag{4.14}$$

and

$$d_4(\mathbf{r}, \beta) = \sqrt{(z_1 - \beta)^2 + (z_2 - 3\beta)^2}. \tag{4.15}$$

These functions can be differentiated and tested using the same method as in Section 4.1 to reveal the level of sensitivity of the distance metric to errors in amplitude. The results for the interior point (β, β) are shown in Table 4.5 for $\mathcal{E}_b/N_0 = 2.0\,\text{dB}$, and Table 4.6 shows the average slope magnitudes for several values of $\mathcal{E}_b/N_0$. The slope magnitudes for the distance metric again have little dependence on the signal-to-noise ratio, but there appears to be more variation among the bit decisions than for phase errors. The second and fourth bits appear to be more sensitive to changes in amplitude than the first and third bits for an interior point. This is also true for the LLR metric, as shown in Tables 3.7 and 3.9.

The average slope magnitudes for metrics that involve a corner point and other exterior point are shown in Tables 4.7 and 4.8. For a corner point, there is little

Table 4.5: Slopes of distance metrics with a gain factor of unity.

z_1	z_2	$D_1'(1)$	$D_2'(1)$	$D_3'(1)$	$D_4'(1)$
1.8881	1.8881	-2.0761	-3.1342	-2.0761	-3.1342
1.0000	2.2559	-1.3151	-3.0088	-2.0000	-4.0000
0.1119	1.8881	-0.1573	-2.5736	-1.2497	-2.9682
-0.2559	1.0000	0.0000	-2.0000	-0.3787	-2.0724
0.1119	0.1119	0.0088	-1.7472	0.0088	-1.7472
1.0000	-0.2559	-0.3787	-2.0724	0.0000	-2.0000
1.8881	0.1119	-1.2497	-2.9682	-0.1573	-2.5736
2.2559	1.0000	-2.0000	-4.0000	-1.3151	-3.0088
Average (magnitude)		0.8982	2.6880	0.8982	2.6880

Table 4.6: Distance metric slope magnitudes for an interior point in a 16-QAM system with a gain factor of unity.

ENR (dB)	$\lvert D_1'(1)\rvert$	$\lvert D_2'(1)\rvert$	$\lvert D_3'(1)\rvert$	$\lvert D_4'(1)\rvert$
2	0.8982	2.6880	0.8982	2.6880
3	0.9253	2.7534	0.9253	2.7534
4	0.9496	2.8054	0.9496	2.8054
5	0.9709	2.8465	0.9709	2.8465
6	0.9895	2.8788	0.9895	2.8788
7	1.0055	2.9043	1.0055	2.9043
8	1.0192	2.9243	1.0192	2.9243
9	1.0309	2.9401	1.0309	2.9401
10	1.0408	2.9526	1.0408	2.9526

variation in sensitivity among bit decisions. This differs from Table 3.10 for the LLR metric, where the slope magnitudes of the first and third bits differ from those of the second and fourth bits. Corner points also appear to be less sensitive to amplitude errors than interior points for the LLR metric, but this is not the case for the distance metric. For other exterior points, there is more variation in slope magnitudes among different bit decisions for the LLR than for the distance metric. In both cases, the third bit has the smallest average slope. It is difficult to determine how these differences affect the performance of these two metrics, but simulations

Table 4.7: Distance metric slope magnitudes for a corner point in a 16-QAM system with a gain factor of unity.

ENR (dB)	$\lvert D_1'(1)\rvert$	$\lvert D_2'(1)\rvert$	$\lvert D_3'(1)\rvert$	$\lvert D_4'(1)\rvert$
2	2.3761	2.1367	2.3761	2.1367
3	2.4256	2.1989	2.4256	2.1989
4	2.4694	2.2562	2.4694	2.2562
5	2.5081	2.3088	2.5081	2.3088
6	2.5425	2.3570	2.5425	2.3570
7	2.5728	2.4012	2.5728	2.4012
8	2.5996	2.4415	2.5996	2.4415
9	2.6234	2.4783	2.6234	2.4783
10	2.6444	2.5118	2.6444	2.5118

Table 4.8: Distance metric slope magnitudes for an other exterior point in a 16-QAM system with a gain factor of unity.

ENR (dB)	$\lvert D_1'(1)\rvert$	$\lvert D_2'(1)\rvert$	$\lvert D_3'(1)\rvert$	$\lvert D_4'(1)\rvert$
2	2.0548	1.9788	1.0792	2.6880
3	2.0553	1.9974	1.1704	2.7534
4	2.0560	2.0120	1.2554	2.8054
5	2.0567	2.0232	1.3330	2.8465
6	2.0573	2.0318	1.4030	2.8788
7	2.0578	2.0384	1.4657	2.9043
8	2.0583	2.0435	1.5215	2.9243
9	2.0587	2.0474	1.5711	2.9401
10	2.0591	2.0504	1.6150	2.9526

show little difference in sensitivity to amplitude errors between the LLR and distance metrics. Simulation results presented in Chapter 5, provide more insight on the effects of phase and amplitude errors on systems using these two soft-decision decoding metrics.

CHAPTER 5
Performance Analysis

5.1 Performance Results for a System with a Phase Error

To further investigate the sensitivity to phase and amplitude errors of M-QAM systems using error-control coding and soft-decision decoding, we determine the packet error probability for an AWGN channel. Information bits are randomly generated and encoded using two error-control coding techniques. Packets are divided into QAM symbols and transmitted over an AWGN channel. The received signals are demodulated with a phase error θ. Each value of θ represents the phase of the transmitted signals, while the receiver is designed as if signals are transmitted with a phase of zero. The received points are decoded using two soft-decision decoding metrics. The packet error probability is shown as a function of ENR for several values of the phase error θ. Also, the required ENR to achieve a packet error probability of 10^{-2} is shown as a function of θ. The effects of a phase error were observed from simulation results to be symmetric about zero, so results are only shown for positive values of θ. Two error-control coding techniques are considered. A rate 1/2 convolutional code with constraint length 7 is used with Viterbi decoding. The generator polynomials for this code are (133,171) in octal. The encoder uses a packet size of 4096 binary code symbols with 2042 information bits and 6 tail bits, so the actual code rate for the encoder is approximately 0.4985. A turbo product code of rate 0.495 [6] is also considered. This three-dimensional code is derived from two (32,26) extended Hamming codes and a (4,3) parity-check code. This code also uses a packet size of 4096 binary code symbols with 2028 information bits [1].

The ENR required to achieve a packet error probability of 10^{-2} is shown in Fig.

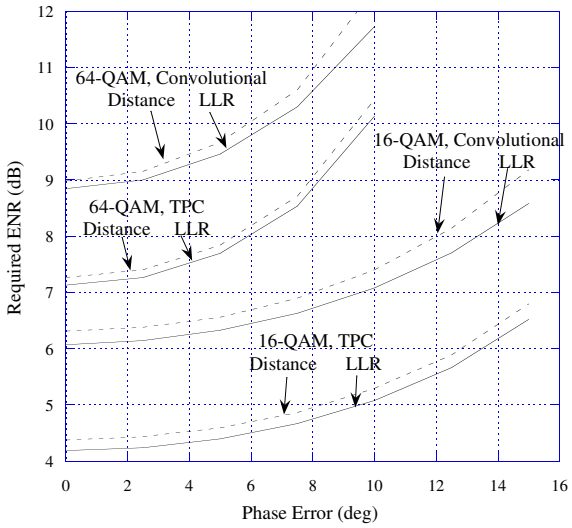

Figure 5.1: Required ENR to achieve a 10^{-2} packet error probability as a function of the phase error

5.1 for the different M-QAM systems considered. The biggest factor in determining phase error sensitivity is the size of the QAM signal set. The curves for 64-QAM are much steeper than those for 16-QAM. The phase error is varied from zero to 10° for 64-QAM and zero to 15° for 16-QAM. Given a 10° phase error, the 64-QAM system requires an ENR approximately 3 dB larger than a system with no phase error. There is very little difference in sensitivity between the two error-control coding techniques or the soft-decision decoding metrics, although there are slight differences for large phase errors. These subtle differences are further examined in Figs. 5.2–5.5.

The packet error probabilities for the 16-QAM system with the convolutional code are shown in Figs. 5.2 and 5.3. For a packet error probability of 10^{-3}, a 16-QAM system with the convolutional code and a 10° phase error requires approximately 1.2 dB higher $\mathcal{E}_b/N_0$ than a system with no phase error. This is true for a system that employs either the LLR or the distance metric. The performance for a 16-QAM system with the turbo product code is shown in Figs. 5.4 and 5.5. With a 10° phase error, this system requires approximately 1.0 dB higher $\mathcal{E}_b/N_0$ for a system employing

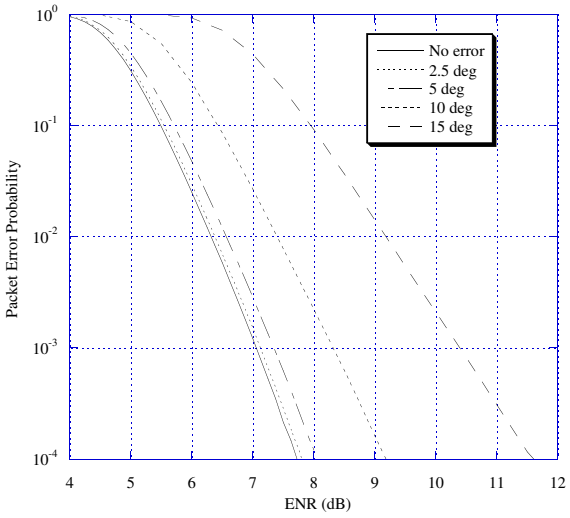

Figure 5.2: Packet error probabilities for several values of the phase error in a 16-QAM system with the convolutional code and the distance metric.

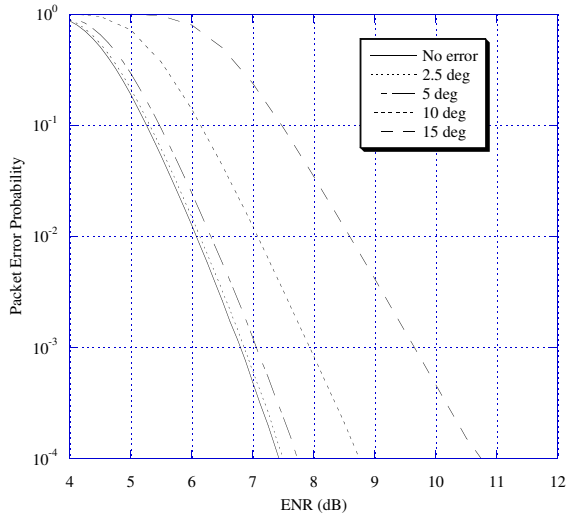

Figure 5.3: Packet error probabilities for several values of the phase error in a 16-QAM system with the convolutional code and the LLR metric.

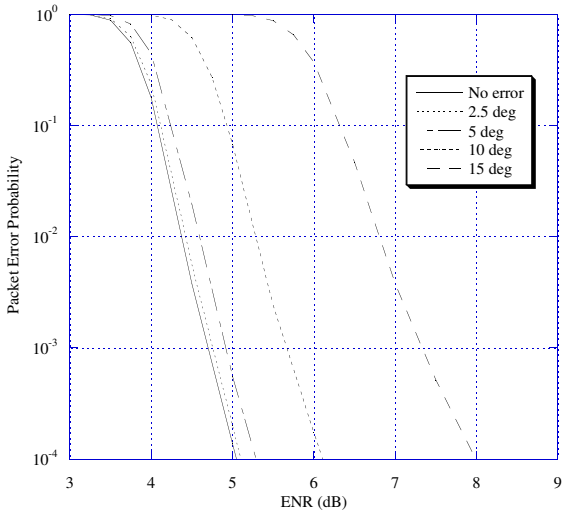

Figure 5.4: Packet error probabilities for several values of the phase error in a 16-QAM system with the turbo product code and the distance metric.

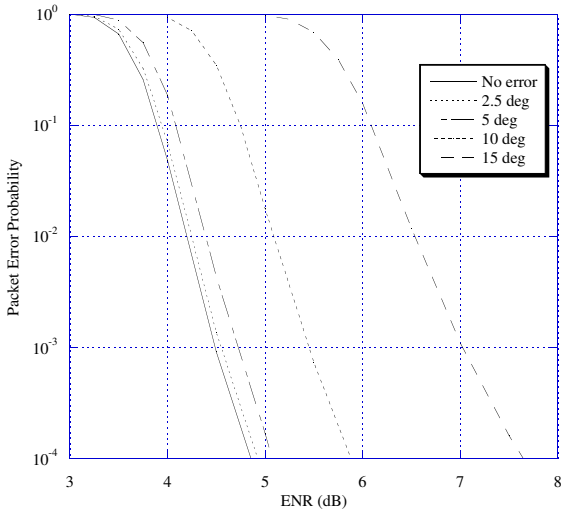

Figure 5.5: Packet error probabilities for several values of the phase error in a 16-QAM system with the turbo product code and the LLR metric.

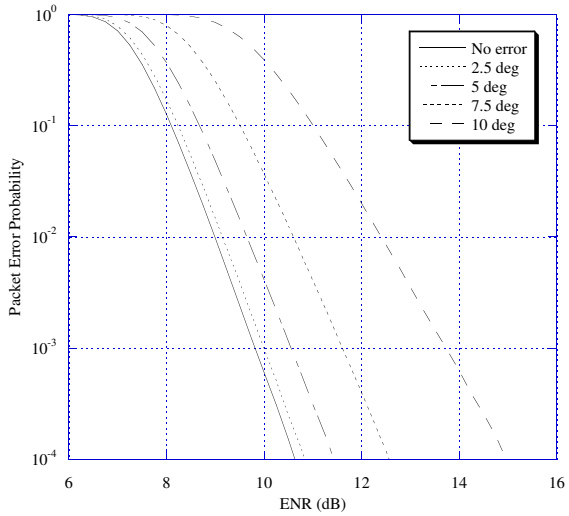

Figure 5.6: Packet error probabilities for several values of the phase error in a 64-QAM system with the convolutional code and the distance metric.

either the LLR or the distance metric. If the phase error is increased to 15°, the effects are much more significant. There is approximately 2.5 dB of performance loss for the system with the turbo product code and approximately 3 dB loss for the system with the convolutional code. The turbo product code shows slightly less sensitivity than the convolutional code for larger phase errors. There is very little difference in sensitivity between the two soft-decision decoding metrics. The biggest difference between the two metrics that we found is for the system with the convolutional code and a 15° phase error. The LLR metric has approximately a 3.0 dB loss while the distance metric has approximately a 3.4 dB loss.

The packet error probabilities for the 64-QAM system with a phase error are shown in Figs. 5.6–5.9. It is clear from these results that a 64-QAM system is more sensitive to phase errors than a 16-QAM system. As observed in the 16-QAM system, there is very little difference in sensitivity between the two soft-decision decoding metrics, and the largest difference is for the system with the convolutional code and a large phase error. It can be seen in Fig. 5.7 that for a packet error probability of 10^{-3},

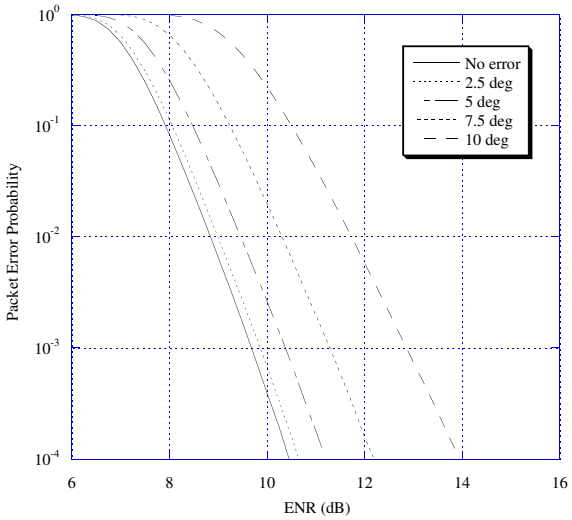

Figure 5.7: Packet error probabilities for several values of the phase error in a 64-QAM system with the convolutional code and the LLR metric.

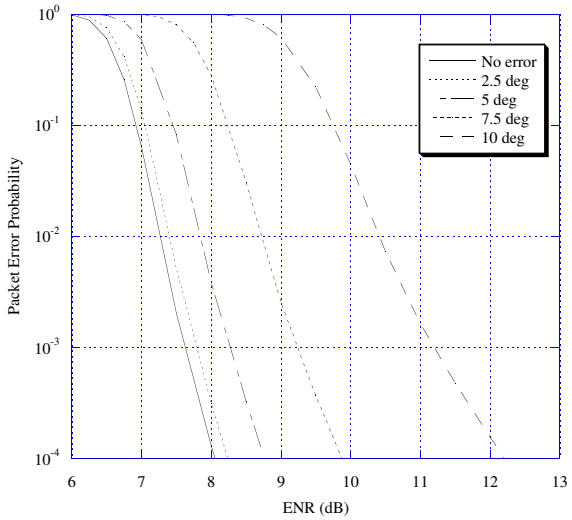

Figure 5.8: Packet error probabilities for several values of the phase error in a 64-QAM system with the turbo product code and the distance metric.

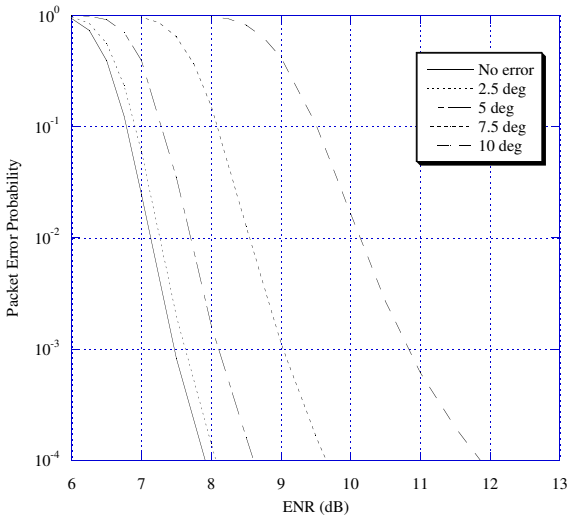

Figure 5.9: Packet error probabilities for several values of the phase error in a 64-QAM system with the turbo product code and the LLR metric.

there is approximately a 3 dB loss in performance for a system with the LLR metric and a 10° phase error. In Fig. 5.6, for the system with the distance metric, there is approximately a 4 dB loss. In both the 16-QAM and 64-QAM systems with the convolutional code and a large phase error, the LLR metric shows less performance degradation than the distance metric.

The LLR metric outperforms the distance metric in all cases. However, the distance metric has the benefit of lower complexity, and it does not require knowledge of the noise variance. There is little difference in sensitivity to phase errors between the two metrics, but the LLR metric was observed to be slightly less sensitive in some cases for large phase errors. The sensitivity also increases as the size of the QAM signal set increases. 64-QAM is much more sensitive to phase errors than 16-QAM for both the LLR and distance metrics and for both the convolutional and turbo product codes. The number of signals in an M-QAM system is the primary factor in determining the sensitivity to a phase error in the system.

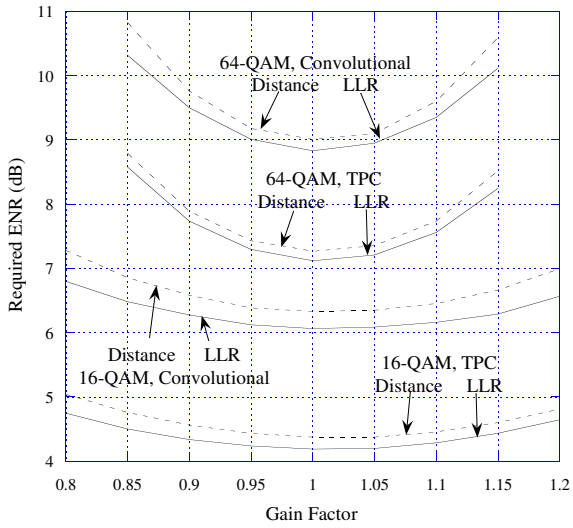

Figure 5.10: Required ENR to achieve a 10^{-2} packet error probability as a function of the gain factor.

5.2 Performance Results for a System with an Amplitude Error

To examine the effects of amplitude errors on the performance of QAM systems, a gain factor of β is applied at the receiver in the performance analysis from Section 5.1. The required ENR to achieve a packet error probability of 10^{-2} is shown as a function of the gain factor in Fig. 5.10. Results are included for the 16-QAM and 64-QAM systems for the two error-control coding techniques and soft-decision decoding metrics considered in Section 5.1.

The performance degradation caused by an amplitude error is not symmetric. Under-estimating the amplitude at the receiver (i.e., $\beta < 1$) causes slightly worse performance than over-estimating by the same amount(i.e., $\beta > 1$), and this can be seen in Figs. 5.10–5.18. In Fig. 5.10, each curve is slightly higher on the left than on the right because under-estimating the amplitude requires a higher value of ENR. It is also clear from Fig. 5.10 that 64-QAM is much more sensitive to amplitude errors than 16-QAM. The curves for 64-QAM are much steeper than the curves for 16-QAM, and for a gain factor of 0.85, the 64-QAM system suffers more than twice

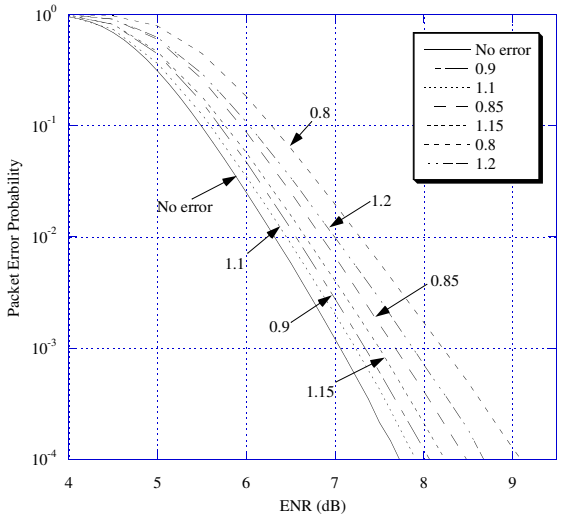

Figure 5.11: Packet error probabilities for several values of β in a 16-QAM system with the convolutional code and the distance metric.

the performance loss of the 16-QAM system.

The packet error probability is shown as a function of ENR for several values of β in Figs. 5.11–5.18. These results also show the reduced penalty of over-estimating compared with under-estimating the amplitude. In each case, under-estimating the amplitude results in a higher packet error probability than over-estimating by the same amount. The LLR metric shows better performance and is also slightly less sensitive to amplitude errors than the distance metric. However, as with phase errors, these differences are subtle and the size of the QAM signal set is the primary factor in sensitivity to amplitude errors. 64-QAM requires more accurate estimates of the amplitude than 16-QAM. In Figs. 5.13 and 5.14, a gain factor of 0.85 in a 64-QAM system requires approximately 2 dB higher ENR to achieve a packet error probability of 10^{-3} versus approximately 0.5 dB for 16-QAM, as seen in Figs. 5.11 and 5.12. There is also very little difference in sensitivity between the two error-control coding techniques. The performance degradation due to amplitude errors in systems with the turbo product code is about the same as the degradation in systems with the

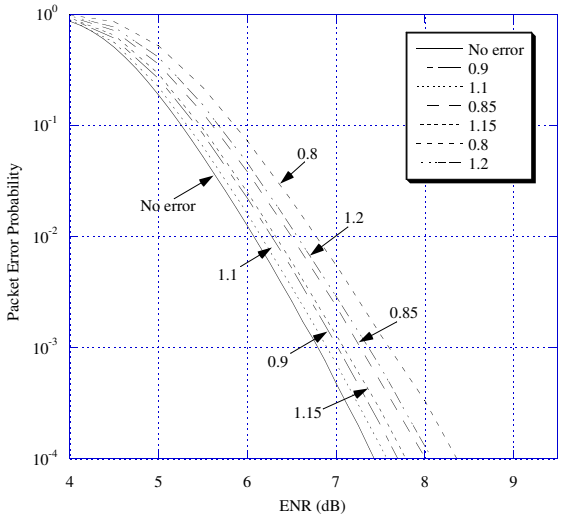

Figure 5.12: Packet error probabilities for several values of β in a 16-QAM system with the convolutional code and the LLR metric.

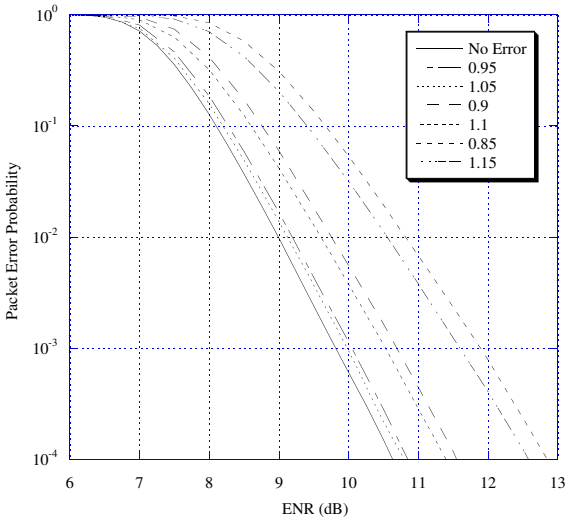

Figure 5.13: Packet error probabilities for several values of β in a 64-QAM system with the convolutional code and the distance metric.

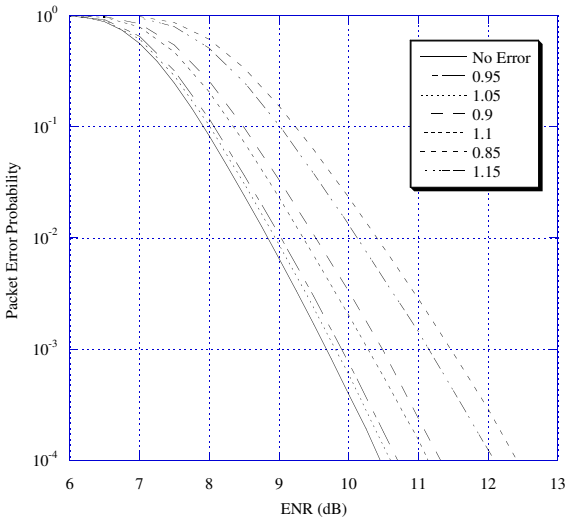

Figure 5.14: Packet error probabilities for several values of β in a 64-QAM system with the convolutional code and the LLR metric.

convolutional code.

In practice, both the phase and amplitude must be estimated. Figures 5.19 and 5.20 show results for a 64-QAM system with both a 5° phase error and a gain factor of 1.1. As expected, an incorrect estimate of both the phase and amplitude causes more performance degradation than an incorrect estimate of either one alone. A 5° phase error or gain factor of 1.1 causes about a 0.5 dB loss in performance in a 64-QAM system; however, the presence of both errors causes over 1 dB of performance loss in the system for both error-control coding techniques and soft-decision decoding metrics.

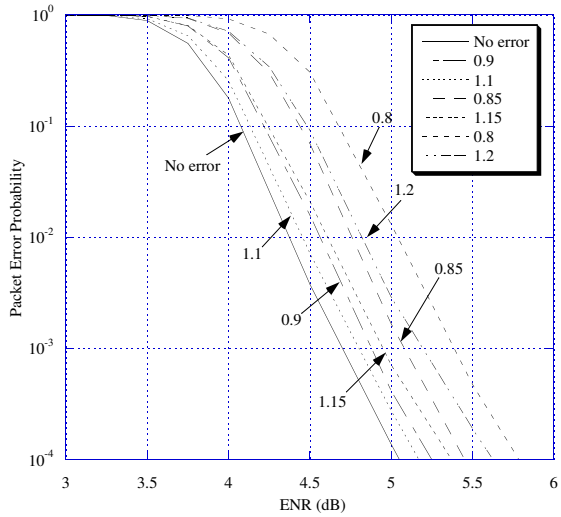

Figure 5.15: Packet error probabilities for several values of β in a 16-QAM system with the turbo product code and the distance metric.

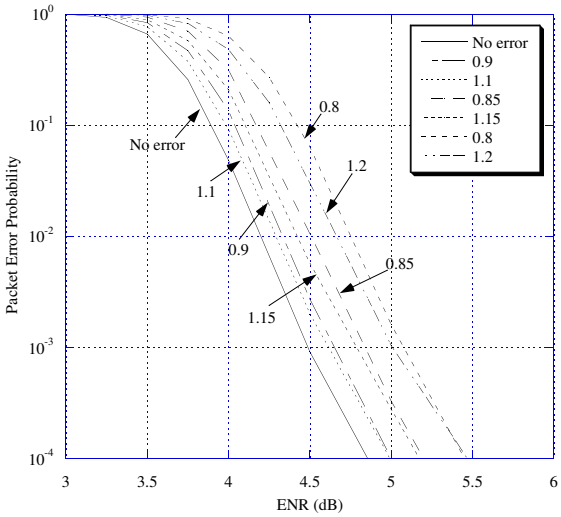

Figure 5.16: Packet error probabilities for several values of β in a 16-QAM system with the turbo product code and the LLR metric.

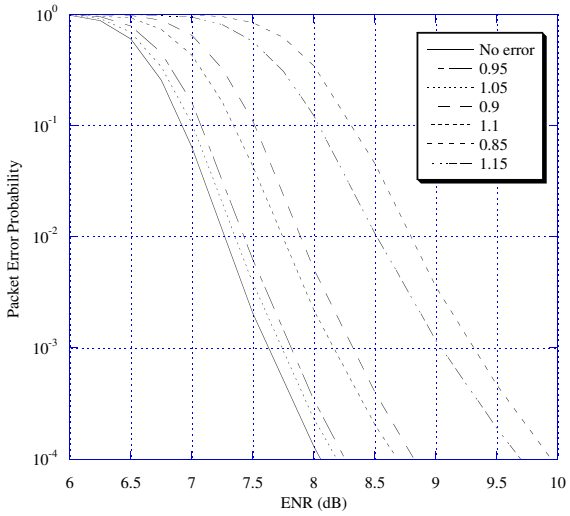

Figure 5.17: Packet error probabilities for several values of β in a 64-QAM system with the turbo product code and the distance metric.

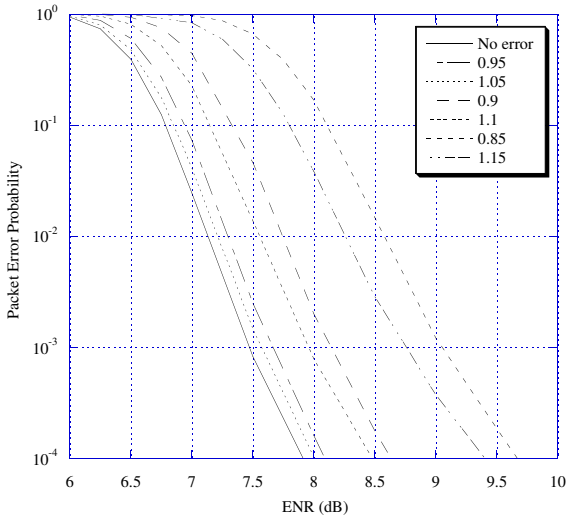

Figure 5.18: Packet error probabilities for several values of β in a 64-QAM system with the turbo product code and the LLR metric.

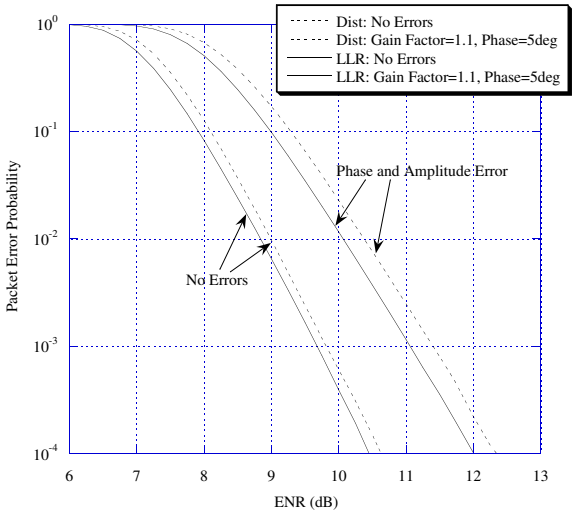

Figure 5.19: Packet error probabilities for a 64-QAM system with phase and amplitude errors using the convolutional code.

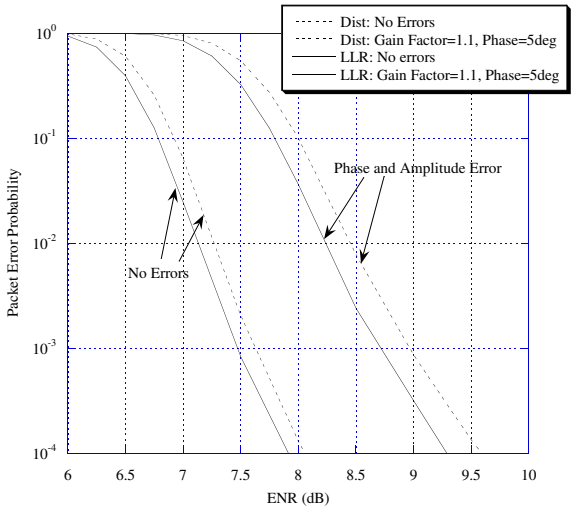

Figure 5.20: Packet error probabilities for a 64-QAM system with phase and amplitude errors using the turbo product code.

CHAPTER 6
Conclusion

Inaccurate estimates of the phase and amplitude of M-QAM signals can cause significant degradation in the performance of the system. Although error-control coding and soft-decision decoding can reduce the effects of phase and amplitude errors, they do not remove them. The log likelihood ratio metric and the distance metric have similar performance in the presence of phase and amplitude errors in an M-QAM system. The LLR metric has a slight advantage for amplitude errors and for large phase errors. The turbo product code has a clear advantage in performance over the convolutional code; however, it does not show a clear advantage in performance sensitivity to phase and amplitude errors. Both error-control coding techniques have about the same degree of sensitivity to such errors. In general, the number of signals in an M-QAM signal set is the primary factor in determining the required accuracy of phase and amplitude estimates. As the size of the signal set increases, more accurate estimates are required and thus more sophisticated techniques for estimating these parameters are required. Under-estimating the amplitude causes slightly worse performance than over-estimating the amplitude by the same amount. This suggests that a positive bias might be used for the amplitude estimates of a QAM signal.

REFERENCES

[1] W. G. Phoel, J. A. Pursley, M. B. Pursley, and J. S. Skinner, "Frequency-hop spread spectrum with quadrature amplitude modulation and error-control coding," *Proceedings of the 2004 IEEE Military Communications Conference* (Monterey, CA), vol. 2, pp. 913–919, November 2004.

[2] M. B. Pursley, *Introduction to Digital Communications*, Upper Saddle River, NJ: Prentice Hall, 2005.

[3] M. K. Simon, S. M. Hinedi, and W. C. Lindsey, *Digital Communication Techniques*, Englewood Cliffs, NJ: PTR Prentice Hall, 1995.

[4] M. K. Simon and J. G. Smith, "Carrier synchronization and detection of QASK signal sets," *IEEE Transactions on Communications*, vol. 22, no. 2, pp. 98–106, February 1974.

[5] Institute of Electrical and Electronics Engineers, *Standard 802.11-2007, Part 11: Wireless LAN Medium Access Control (MAC) and Physical Layer (PHY) Specifications*, June 2007. Available: http://standards.ieee.org/getieee802/download/802.11-2007.pdf

[6] Advanced Hardware Architectures, Inc., Product Specification for AHA4501 Astro 36 Mbits/sec Turbo Product Code Encoder/Decoder. Available: http://www.aha.com